Tension-driven cracking of an expanded austenite layer

B. A. LATELLA*, K. T. SHORT
Materials and Engineering Science, Australian Nuclear Science and Technology Organisation, PMB 1, Menai, NSW 2234, Australia
E-mail: bal@anto.gov.au

Protective layers and coatings need to retain their integrity when subjected to external loads and impacts because incipient cracking and damage can result in delamination and spalling to expose the underlying material. Characterizing the damage evolution and adhesion performance of these coating–substrate systems to externally applied stresses is important when planning engineering applications. One such material system is expanded austenite, which is a nitrided layer of stainless steel. It has received considerable attention as a protective layer due to the combination of high hardness, stiffness, and wear resistance it provides to the underlying compliant and soft austenitic stainless steel surface [1–3]. The nature and structure of expanded austenite has been the subject of debate for some time [2, 4–6] with work conducted in our laboratory [7] suggesting that it is crystalline and dominated by a cubic phase with considerable expansion of the austenite lattice. It may also contain precipitates of CrN and α-Fe that vary in size and quantity depending on the nitriding temperature. The expansion of the austenite lattice yields high compressive stresses, which conveys that the wear resistance and the high hardness of the layer is due to high dislocation density [8]. The consequences of this hard, highly stressed layer and its contribution to the mechanical stability and durability of the system will be addressed.

Accordingly, the present study investigates the mode of damage in an expanded austenite layer on stainless steel when subjected to monotonic tensile loading. Optical microscopy was used to characterize and quantify the observed cracking and damage evolution during loading. We will find that the damage is confined to the expanded austenite layer and is characterized by many parallel cracks extending along as well as through the entire layer ending abruptly at a distinct interface with the substrate. There is no delamination or spalling of the layer indicating excellent interfacial bonding.

As-received stainless steel (type AISI 316) sheeting, nominally 0.6 mm thick, was cut into small tensile samples (length = 33 mm, width = 3 mm and gauge length = 12 mm). The surface on one face of each sample was routinely polished to a 1 μm finish. The polished face of each sample was then nitrided using plasma immersion ion implantation (PI^3) in pure N_2 at 420 °C for 5 h with a pulsed high voltage bias of -30 kV (pulse = 100 μs with a duty cycle of 2%). The plasma was generated with an rf discharge. Further details of the method can be found in [9]. The thickness of the modified layer was determined from a polished cross-section etched with Marble's reagent (4 g $CuSO_4$, 20 ml HCl, 20 ml H_2O). The thickness of the layer was found to be quite uniform over the length of the sample at $\approx$12 μm. The stress in the layer was calculated using Stoney's equation [10] by measuring the curvature of all the samples before and after nitriding with a stylus profilometer. The residual stress in the layer was found to be highly compressive and of the order of -1.6 ± 0.23 GPa. A nanoindenter (Nano instruments—NANO IIs indenter system) was used to measure the hardness (H) and Young's modulus (E_f) of the expanded austenite layer. At least five indentations were made with a Berkovich indenter using a peak load of 50 mN. The average hardness of the expanded austenite was found to be 21 ± 1.5 GPa (compared to stainless steel $H = 1.73$ GPa) while its Young's modulus was 320 ± 8 GPa (ca. stainless steel $E = 208$ GPa).

Examination of the cracking damage was made using tensile tests with a small mechanical testing device equipped with a 2500 N capacity load cell and an LVDT to measure displacement. The flat nitrided stainless steel samples were attached to the instrument holder and then positioned directly under the objective lens of an optical microscope (Zeiss Axioplan) at a fixed magnification and pulled uniaxially at a rate of 0.005 mm/s. This allowed direct observation of crack initiation and evolution in the expanded austenite layer. The applied load and the imposed displacement were recorded during the tests. Simultaneously optical images of the surface were acquired using an analog camera with image analysis software (Scion Image, NIH).

Fig. 1 shows a selection of optical images of the expanded austenite surface during tensile loading at various strains demonstrating the evolution of cracking. Fig. 1a shows the starting surface of the expanded austenite just prior to loading (0% strain). The microstructure consists of grains averaging about 30 μm in size with twinning evident within individual grains due to the highly stressed layer. The nucleation of cracking occurs at a strain of 1.85%, and Fig. 1b shows a crack extending from a region at the lower left of the image in a perpendicular direction to the tensile axis at a strain of 1.97%. This crack was observed to proceed in both directions from a defect near a grain boundary junction at an estimated velocity of 75 μm/s. Fig. 1c shows the evolution of several parallel cracks in the

* Author to whom all correspondence should be addressed.

0022–2461 © *2004 Kluwer Academic Publishers*

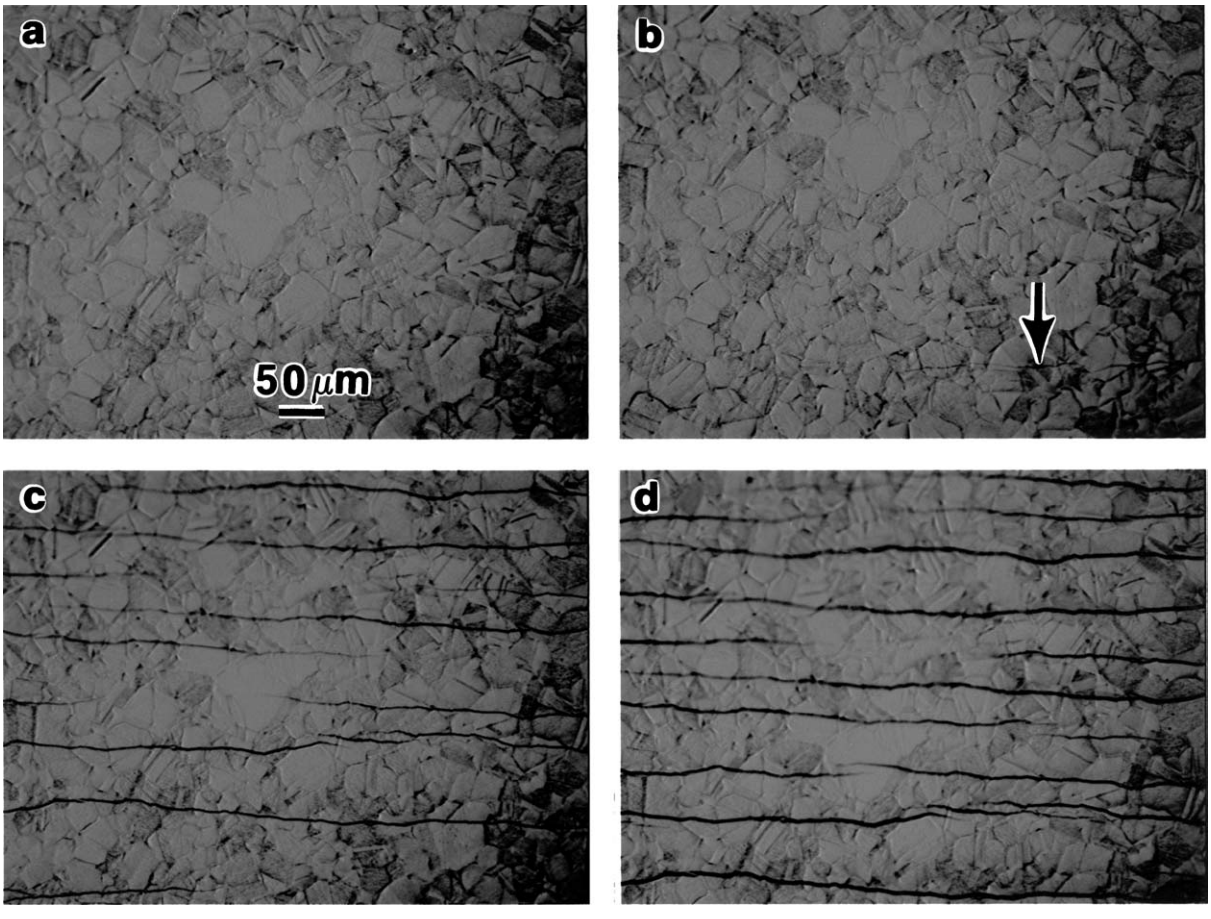

Figure 1 Optical micrographs of the damage observed in the expanded austenite layer during tensile loading for (a) 0%, (b) 1.97% (arrow points to first transverse crack), (c) 4.5% and (d) 8.3% strain. Loading is in the vertical direction.

expanded austenite layer at a strain of 4.5%. Finally, Fig. 1d shows the fully developed parallel cracks at a strain of 8.3%, which corresponded to the end of the test.

The classical parallel cracking observed in the expanded austenite layer, transverse to the loading direction and normal to the interface, is consistent with observations in other fracture studies of brittle coatings on ductile substrates [11–13]. The pertinent features of the damage produced reveal that the length of the parallel cracks increase, and the density of these cracks becomes considerably more pronounced with strain to a saturation level as illustrated graphically in Fig. 2. At the saturation level the extensive array of parallel cracks that predominate in the layer throughout the entire gauge length of the specimen are regularly spaced at about 60 μm (see Fig. 1d). The intercrack spacing reduces in extent during loading as shown in the sequence of images in Fig. 1 to a point beyond which no further cracking of the layer is possible corresponding to the crack density saturation level. The spacing of these cracks is dictated by shear load transfer from the cracked layer to the substrate [12, 14].

From the experiments it was then possible to calculate fracture parameters of the coated system. Assuming an elastic response, the critical stress for cracking, σ_c, of the expanded austenite layer was obtained taking into account the effect of the residual stress, σ_r (i.e.,

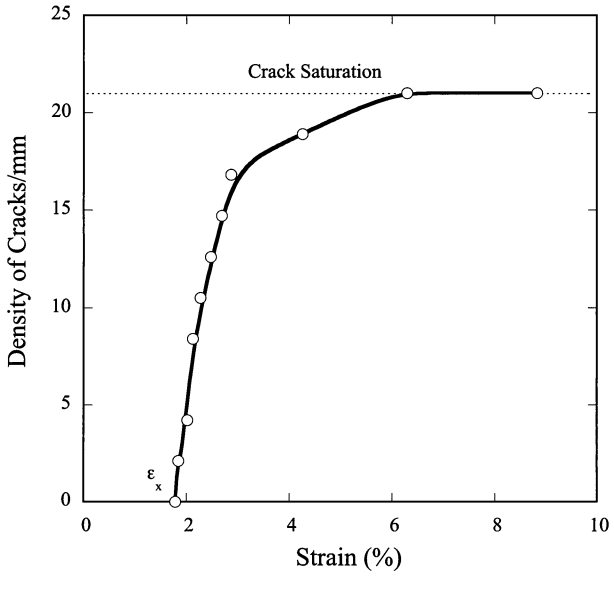

Figure 2 Evolution of transverse cracking density as a function of longitudinal strain of the stainless steel substrate.

$\varepsilon_r = \sigma_r/E_f = -0.5\%$):

$$\sigma_c = (\varepsilon_x + \varepsilon_r)E_f \quad (1)$$

where E_f is the Young's modulus of the coating, and the critical strain for the first cracking of the expanded austenite layer is $\varepsilon_c = \varepsilon_x + \varepsilon_r = 1.35\%$, with

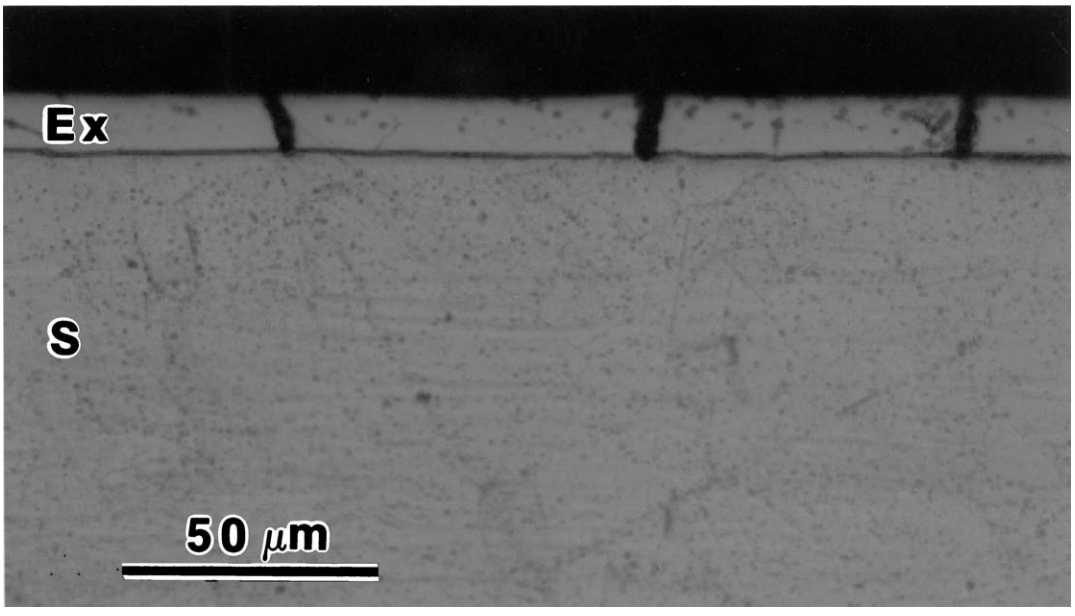

Figure 3 Optical image of an etched cross-section of a sample deformed to a maximum strain of 8.3% (the corresponding surface image is Fig. 1d). The labels Ex denotes expanded austenite layer and S denotes the substrate. Note the dark CrN precipitates in the expanded austenite layer.

$\varepsilon_x (= 1.85\%)$ the strain for the first cracking observed in the tensile test and ε_r the residual strain. The layer fracture toughness (K_{IC}) is given by [15]

$$K_{IC} = \left(\sigma_c^2 t \left[\pi F(\alpha_D) + \frac{\sigma_c}{\sqrt{3}\sigma_Y} \right] \right)^{1/2} \quad (2)$$

and the interfacial fracture energy (γ_i) is

$$\gamma_i = \frac{1}{2} E_f t \varepsilon_i^2 \quad (3)$$

where t is the layer thickness, $F(\alpha_D)$ is a function of the elastic contrast between layer and substrate [16] and σ_Y is the yield stress of the substrate (obtained from a tensile experiment on an as-received stainless steel coupon, $\sigma_Y \approx 300$ MPa). From these equations we find that $\sigma_c = 4.31$ GPa and $K_{IC} = 51$ MPa·m$^{1/2}$. The absence of delamination of the layer even at the maximum strain of 8.3% enabled a lower bound value to be given for the interfacial fracture energy, i.e., $\gamma_i \gg 10180$ Jm^{-2} ($K_{IC} = 57$ MPa·m$^{1/2}$), which is noticeably larger than the layer toughness. For comparison, the fracture toughness for high-alloy steels is $K_{IC} = 50$ to 170 MPa·m$^{1/2}$ and for mild steel, 140 MPa·m$^{1/2}$ [17].

Fig. 3 shows a polished and etched cross-section of a tested sample (strain = 8.3%) with the cracks penetrating through the entire layer to the interface with the stainless steel. It appears most likely that the cracks induce localised plastic flow in the substrate to occur. The effect of the plastic flow in the substrate is to blunt the crack tip at the interface and inhibit longitudinal de-adhesion of the layer. The distinct line delineating the layer with stainless steel is due to the etching, as confirmed from examination of the microstructure in adjacent unetched regions. Hence the intersection and blunting of these transverse cracks at the interface illustrates the excellent interfacial bonding and adhesion of the system. Also noticeable within the expanded austenite layer is a scattering of small, dark areas identified from energy dispersive spectroscopy as CrN precipitates. Interestingly these hard CrN precipitates appear to have no effect on the cracking damage observed in the layer.

It has been shown that for monotonic tensile loading, expanded austenite cracking is the predominant damage mode. The cracking of the layer starts at a strain of 1.85%, which is well within the plastic deformation region of stainless steel. Debonding and spalling of the layer was not observed, indicating excellent interfacial adhesion. Overall the expanded austenite layer provides an adequate protective barrier on austenitic steels, but cracking of this layer (above a critical strain) has a profound effect on material behaviour and susceptibility to accelerated degradation in monotonic loading, which needs to be considered in design and application of the system. Further detailed fracture studies to ascertain the influence of nitriding temperature on cracking damage will be presented elsewhere.

Acknowledgments

The authors would like to thank S. Humphries and G. Smith for assistance with sample preparation.

References

1. Z. L. ZHANG and T. BELL, *Surf. Eng.* **1** (1985) 131.
2. M. SAMANDI, B. A. SHEDDEN, D. I. SMITH, G. A. COLLINS, R. HUTCHINGS and J. TENDYS, *Surf. Coat. Tech.* **59** (1993) 261.
3. C. BLAWERT, A. WEISHEIT, B. L. MORDIKE and F. M. KNOOP, *ibid.* **85** (1996) 15.
4. G. A. COLLINS, R. HUTCHINGS, K. T. SHORT, J. TENDYS, X. LI and M. SAMANDI, *ibid.* **74/75** (1995) 417.
5. M. P. FEWELL, D. R. G. MITCHELL, J. M. PRIEST, K. T. SHORT and G. A. COLLINS, *ibid.* **131** (2000) 300.
6. X. LI, M. SAMANDI, D. DUNNE and R. HUTCHINGS, *ibid.* **71** (1995) 175.

7. D. R. G. MITCHELL, D. J. ATTARD, G. A. COLLINS and K. T. SHORT, *ibid.* **165** (2003) 107.
8. K. L. DAHM and P. A. DEARNLEY, *Proc. Inst. Mech. Eng.* **214** (2000) 181.
9. G. A. COLLINS, R. HUTCHINGS, K. T. SHORT, J. TENDYS and C. H. V. D. VALK, *Surf. Coat. Tech.* **84** (1996) 537.
10. G. G. STONEY, *Proc. Roy. Soc. Lond.* A **82** (1909) 172.
11. M. IGNAT, T. MARIEB, H. FUJIMOTO and P. A. FLINN, *Thin Solid Films* **353** (1999) 201.
12. P. SCAFIDI and M. IGNAT, *J. Adhesion Sci. Tech.* **12** (1998) 1219.
13. B. A. LATELLA, M. IGNAT, C. J. BARBÉ, D. J. CASSIDY and J. R. BARTLETT, *J. Sol-Gel Sci. Tech.* **26** (2003) 765.
14. J. S. WANG, Y. SUGIMURA, A. G. EVANS and W. K. TREDWAY, *Thin Solid Films* **325** (1998) 163.
15. M. IGNAT, *Key Eng. Mat.* **116/117** (1996) 279.
16. J. L. BEUTH and N. W. KLINGBEIL, *J. Mech. Phys. Solids* **44** (1996) 1411.
17. M. F. ASHBY and D. R. H. JONES, "Engineering Materials 2: An Introduction to Microstructures, Processing and Design" (Pergamon Press, Oxford, 1986).

Received 12 November
and accepted 30 December 2003